Calculation of Heating of Passive Implants by the RF Electromagnetic Field in MRI

J.A. Nyenhuis and C.R. Miller

Purdue University, School of Electrical and Computer Engineering, 465 Northwestern Avenue, West Lafayette, Indiana 47907 USA, nyenhuis @purdue.edu; mille352@purdue.edu

Abstract

The in-vitro and in-vivo temperature rises during MRI for a sample passive implant in the form of a metal rod of 8 mm diameter and 118 mm length in the right humerus were calculated with FDTD and the heat equation. The temperature rise in a phantom test was calculated for a background medium with electric properties specified in ASTM F2182-09 and for a medium with electrical properties of the cancellous bone that surrounds the implant. Scaled to local background SAR, in-vitro rises are greater for the bone. For a patient in the MRI coil with landmark in the torso and a whole body SAR of 2 W/kg, the calculated temperature rise after six minutes of RF power deposition was 1.3 °C for 64 MHz and 2.4 °C for 128 MHz. The numerical methods presented here could be extended to determine the temperature rises that would occur in the phantom and in the patient for other implants.

1. Introduction

ASTM F2182-09 [1] is a standard for testing of heating of passive implants. The implant to be tested is placed in a phantom, temperature probes are placed on or near the implant, the implant and phantom assembly are placed in the MRI coil, and RF power is applied to the coil. Temperature vs. time is recorded with fiber optic temperature probes. The standard intends to produce a measurement that yields the greatest possible temperature rise by situating the implant in the region of phantom where the background electric field is most intense and by placement of the temperature probes at locations on or near the implant that heat the most. For complex implants it may not be clear where the heating will be the greatest.

The temperature rise of an implant in the patient will depend on the electric field direction and intensity in its vicinity, as well as the electrical properties of the surrounding tissues. The phantom described in ASTM F2182-09 is rectangular and contains a single medium with conductivity (0.47 S/m) and relative dielectric constant (about 80) that approximate average values for human tissue. Furthermore the distribution of electric field in the phantom is different than in the human. The temperature rises for an implant in a phantom test will thus provide only an approximate indication of the heating that will occur in the patient.

We here present methods for the calculation of the in-vitro and in-vivo heating of a passive implant. This work was motivated by the need to identify the location of greatest heating in a phantom test and by the need to more accurately determine the temperature rise in the patient.

2. Methods

The electric fields were calculated with the Finite Difference Time Domain Method (FDTD). The MRI coils were high pass birdcages with length and diameter of 64 cm. Voltages were applied between the arms at the end rings to produce the circularly polarized incident RF fields. In-vitro simulation of the heating of the model implant that would occur in a phantom test was calculated with a plane wave simulator. The implant was placed in the center of rectangular box in a uniform medium. Plane waves were launched from opposite walls of the box to produce an approximately uniform electric field along the length of the implant.

The Hugo model was used for the in-vivo calculations. This model was derived from the Visible Human Project at the US National Library of Medicine and has frequently been used in MRI calculations. The Huygens box method was used for the calculation of the electric field in the portion of the human model containing the implant. [2]. In a first FDTD simulation, the electric fields for the patient in the coil were calculated for a uniform resolution of 5 mm. A section of the Hugo model containing the implant with variable gridding ranging from 0.35 mm to 1.5 mm was defined. The boundary conditions on the box for the second FDTD calculation were the tangential components of the magnetic and electric fields from the coarse resolution simulation.

The electric fields intensity E (units V/m) is here defined to be the amplitude of a continuous wave. The Specific Absorption Rate (SAR) is then

978-1-4244-6051-9/11/$26.00 ©2011 IEEE

$$SAR = \frac{\sigma E^2}{2\rho} \quad (1)$$

where σ is the conductivity in S/m and ρ is the mass density in kg/m^3. The temperature rise was calculated with the heat equation by time integration of the SAR and utilizing the thermal properties of titanium alloy for the implant.

3. Results

Figure 1 shows the SAR distribution in a uniform medium for a model implant in the form of a 8 x 118 mm titanium rod and the corresponding temperature rise after six minutes of heating. The electric field is a plane wave polarized along the Z axis, which approximates the configuration of a passive implant placed inside the phantom in a longitudinal orientation. There is an intense SAR concentration that approaches 100 times the background at the ends of the rod. The temperature rise vs. time has a decreasing slope and this slope depends on the location of the probe.

Table 1 lists the calculated temperature rises for the titanium rod in the plane wave model at 64 MHz and 128 MHz. The rod was placed in the phantom medium (Gel) and inside cancellous bone. The greatest temperature rise at both frequencies occurs in cancellous bone. It is noteworthy that the temperature rise is smaller at 128 MHz than 64 MHz for the phantom medium, while the opposite is true for the rod inside cancellous bone. This is because the wavelength is longer in cancellous bone owing to lower dielectric constant.

Table 1. Calculated in-vitro rises scaled to a local background SAR of 1 W/kg.

Frequency (MHz)	Medium	Background σ	Background ε_r	Power time (min)	ΔT (°C)
64	Gel	0.47	78	6	1.18
64	Cancellous bone	0.16	31	6	1.40
128	Gel	0.47	78	6	0.80
128	Cancellous	0.16	31	6	1.63

Figure 2 shows the placement of the implant in the patient. It is centered inside the humerus and is located between z=0.30 m and 0.41m. In the absence of the rod, the electric field intensity near the end at z=0.41 m is about 100 V/m. With the rod, the electric field increases nearly 4-fold. There is also intense electric field in the fat due to its lower electrical conductivity compared to muscle and other tissues.

Figure 3 shows the electric field intensity for the Hugo model in RF coil at 128 MHz at a whole body SAR (WB SAR) of 2 W/kg. The path of the implant in the humerus is indicated by the dark line. The background tangential electric field E_{tan} along the path of the implant is also shown in Fig. 3. For the WB-SAR of 2 W/kg, the spatial rms of E_{tan} along the path is 129 V/m. For 64 MHz, the corresponding value is 109 V/m.

Figure 4 shows the placement of the implant in the cancellous bone and the corresponding distribution of the calculated temperature rise at 64 MHz and 128 MHz. The rise after six minutes is 1.34 °C at 64 MHz and 2.41 °C at 128 MHz. These values were calculated without perfusion. While the pattern of the temperature rise surrounding the end of the rod is similar for both frequencies, temperature rise is greater at 128 MHz.

The in-vivo temperature rise at the end of the rod can be estimated by scaling the in-vitro rises for cancellous bone from Table 1 by the average in-vivo tangential SAR, which is obtained by setting E to E_{tan} in Eq. 1. For a whole body SAR of 2 W/kg, the average tangential SAR along the path of the rod in the humerus is 0.95 W/kg at 64 MHz and 1.33 W/kg at 128 MHz. The predicted in-vivo rises based on Table 1 are then 1.33 °C at 64 MHz and 2.16 °C at 128 MHz. These agree to within 10% with the calculated temperature rises in Fig. 4. Less good agreement is expected if there is significant non-uniformity in background electric field, as the sensitivity of the rod heating to E_{tan} is non-uniform along its length. The transfer function method could be used to account for the heating of the implant due to the distribution of the tangential electric field along its length. [3]

4. Summary and Conclusions

We have demonstrated that it is possible to calculate the RF induced temperature rise for passive implants, both in-vitro and in-vivo. The method is extendable to implants with minimum feature dimension that is an appropriate multiple of the minimum grid spacing in the calculation.

The in-vitro calculations help to identify the locations of greatest heating on the implant in phantom test. It may be possible to reduce the number of tests required to characterize implant heating. The background material can also be adjusted in the calculation to more closely resemble the material surrounding the implant in-vivo.

A merit of the computational approach is that the in-vivo temperature rises can be determined. We have demonstrated that the results obtained in the evaluation of RF-induced heating in accordance with F2182-09 do not necessarily extend to the in-vivo environment. The greater clinical relevance of these in vivo calculations may be to guide a more accurate determination of MRI safety for passive implants.

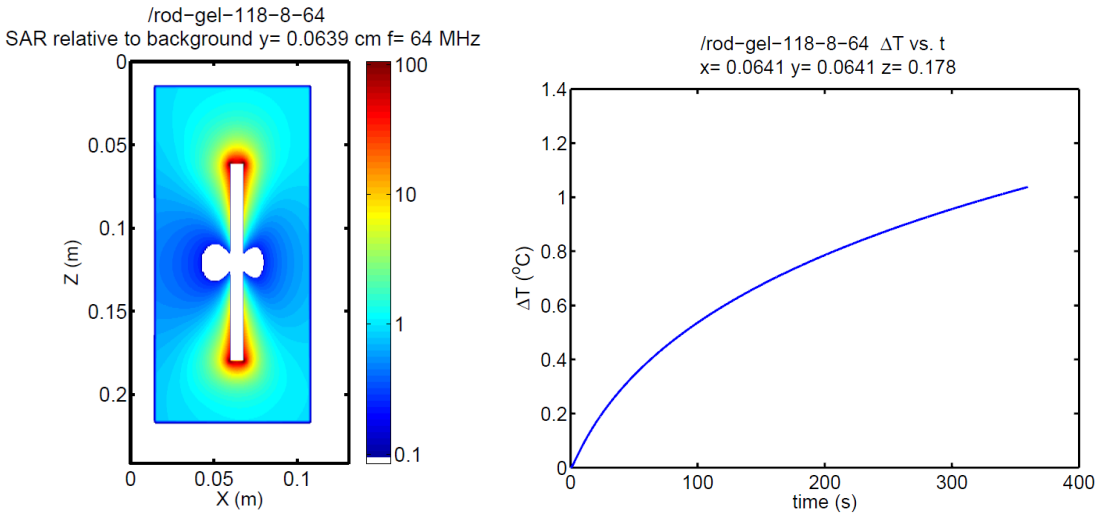

Figure 1. 8 mm diameter × 118 mm long rod in medium with σ= 0.47 S/m and ε_r = 31 with 64 MHz background electric field. Left is SAR distribution and right is temperature rise vs. time at the end of the rod for local background SAR of 1 W/kg.

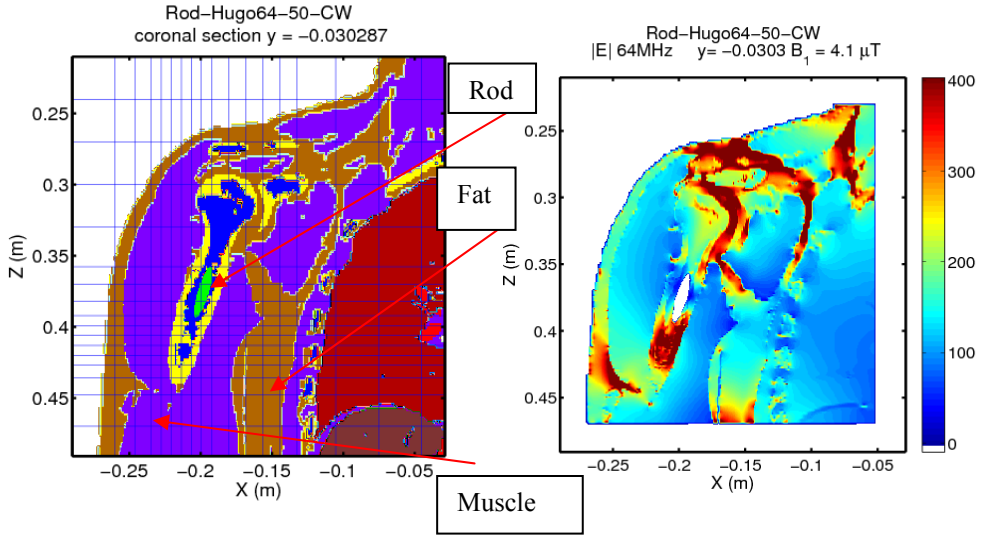

Figure 2. Section of the Hugo model with rod (green) in humerus (left) and electric field distribution (right) at 64 MHz for whole body SAR of 2 W/kg.

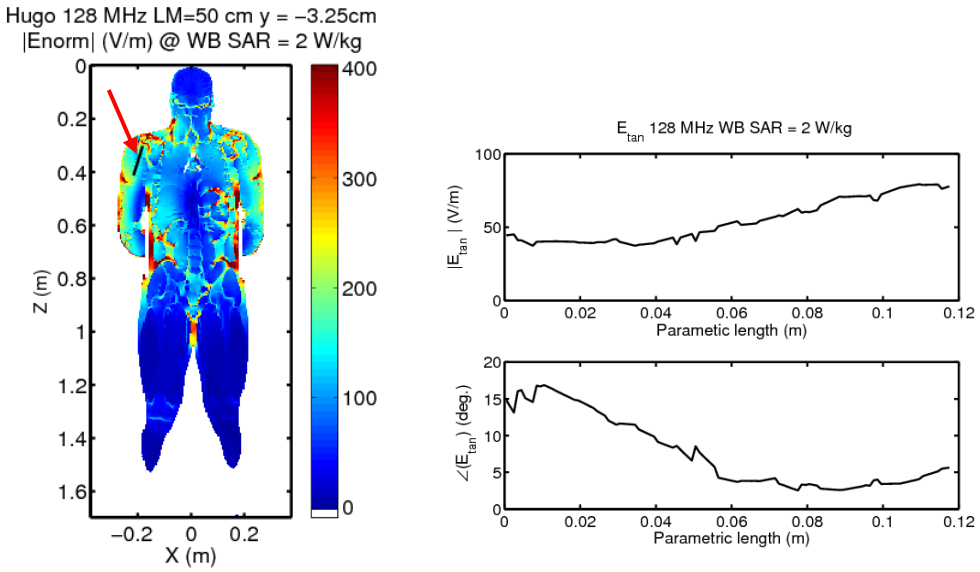

Figure 3. Electric field intensity for Hugo model in RF coil at 128 MHz, with path for the rod in humerus indicated by dark line, highlighted by red arrow. Right plot shows magnitude and phase of tangential electric field along the path of the rod. Whole body SAR is 2 W/kg.

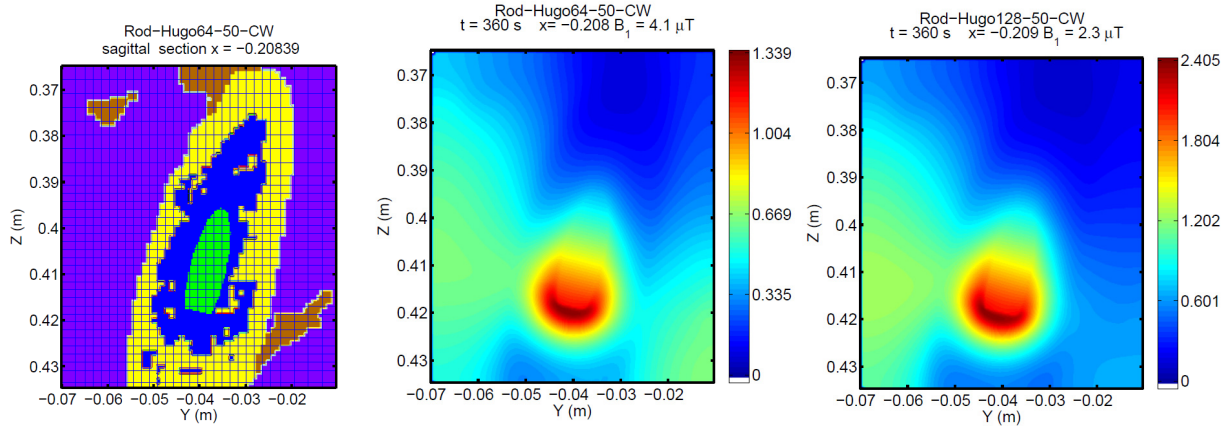

Figure 4. Section of Hugo model at end of rod and corresponding temperature rise distributions at 64 MHz and 128 MHz. Whole body SAR is 2 W/kg and RF power application time was 6 minutes.

5. References

1. ASTM International. Standard test method for measurement of radio frequency induced heating near passive implants during magnetic resonance imaging. ASTM Standard F2182–09 West Conshohocken, PA: ASTM International; 2009. www.astm.org

2. E. Neufeld, S. Kuehn, G. Szekely, and N. Kuster, Measurement, simulation and uncertainty assessment of implant heating during MRI, Phys. Med. Biol. 54:4151-4169, 2009.

3. S.M. Park, R. Kamondetdacha, and J.A. Nyenhuis, Calculation of MRI-Induced Heating of an Implanted Medical Lead Wire With an Electric Field Transfer Function, J. Mag. Reson. Imag., 1278-1285, 2007.